

WildFake: A Large-scale Challenging Dataset for AI-Generated Images Detection

Yan Hong^{1*}, Jianming Feng^{1*}, Haoxing Chen¹

Jun Lan¹, Huijia Zhu¹, Weiqiang Wang¹, Jianfu Zhang^{2†}

¹ Ant Group, ² Qing Yuan Research Institute, Shanghai Jiao Tong University

¹ yanhong.sjtu@gmail.com, hx.chen@hotmail.com

¹ {fengji.fjm, yelan.lj, huijia.zhj, weiqiang.wwq}@antgroup.com

² c.sis@sjtu.edu.cn

Abstract

The extraordinary ability of generative models enabled the generation of images with such high quality that human beings cannot distinguish Artificial Intelligence (AI) generated images from real-life photographs. The development of generation techniques opened up new opportunities but concurrently introduced potential risks to privacy, authenticity, and security. Therefore, the task of detecting AI-generated imagery is of paramount importance to prevent illegal activities. To assess the generalizability and robustness of AI-generated image detection, we present a large-scale dataset, referred to as WildFake, comprising state-of-the-art generators, diverse object categories, and real-world applications. WildFake dataset has the following advantages: 1) Rich Content with Wild collection: WildFake collects fake images from the open-source community, enriching its diversity with a broad range of image classes and image styles. 2) Hierarchical structure: WildFake contains fake images synthesized by different types of generators from GANs, diffusion models, to other generative models. These key strengths enhance the generalization and robustness of detectors trained on WildFake, thereby demonstrating WildFake’s considerable relevance and effectiveness for AI-generated detectors in real-world scenarios. Moreover, our extensive evaluation experiments are tailored to yield profound insights into the capabilities of different levels of generative models, a distinctive advantage afforded by WildFake’s unique hierarchical structure.

1. Introduction

The development of generative models has markedly improved the creation of realistic images, simplifying the

process of producing AI-generated images (*i.e.*, fake images). This heightened accessibility has amplified concerns regarding the widespread spread of false information. AI-generated images, characterized by their striking visual clarity, are particularly persuasive and have the potential to significantly influence public opinion in critical domains such as politics and economics. To counteract such harmful activities, the development of technologies capable of detecting altered images is essential. Generative models typically imprint unique patterns, which don’t appear in real images and vary depending on the model and its training data [49]. Recent research in synthetic image detection has focused on identifying these irregularities through methods like color pattern analysis, light intensity evaluation, and Fourier spectrum analysis [13, 20]. While traditional techniques based on manually selected features and frequency analysis show limited efficacy, deep CNN models are more effective in pattern detection [48]. However, with the range of models available—from Generative Adversarial Networks (GANs) [3, 8, 12, 19, 36, 38, 53, 63, 68, 69] to Diffusion Models (DMs) [59, 62], users can now easily produce high-quality and diverse images with different types of model with personalized weights, and spread those generated images with different social media platforms. These images, often disseminated across various social media platforms, present a significant challenge in terms of generalization and robustness for detection technologies. Existing detectors still face difficulties with generative models not encountered during their training phase [1, 47, 75, 77].

To aid in the development of detectors, many datasets for general AI-generated images are built [7, 55, 66, 71, 74–76, 84]. However, these existing datasets often exhibit significant limitations. They are generally restricted to one or two types of generators, constrained to producing images within fixed categories, or largely dependent on low-

*Equal contribution.

†Corresponding author.

Table 1. Comparison among our WildFake dataset and existing fake image detection datasets.

Datasets	Generators			Communities	Available	Hierarchies	Image Numbers	
	GANs	DMs	Others				Fake	Real
CNNSpot [74]	✓	✗	✗	✗	✓	✗	362,000	362,000
IEEE VIP Cup [71]	✓	✓	✗	✗	✗	✗	7,000	7,000
DE-FAKE [66]	✗	✓	✗	✗	✗	✗	20,000	60,000
CiFAKE [7]	✗	✓	✗	✗	✓	✗	60,000	60,000
GenImage [84]	✓	✓	✗	✗	✓	✗	1,331,167	1,350,000
DiffusionDB [76]	✗	✓	✗	✓	✓	✗	14,000,000	0
ArtiFact [55]	✓	✓	✗	✗	✓	✗	1,521,900	962,200
DiffusionForensics [75]	✗	✓	✗	✗	✓	✗	439,020	92,000
WildFake	✓	✓	✓	✓	✓	✓	2,557,278	1,013,446

quality, user-generated images. These constraints hinder the effectiveness and adaptability of detectors in recognizing a broader range of AI-generated content. In this paper, we present WildFake, a comprehensive, large-scale dataset specifically designed for the detection of AI-generated images. We summarize the comparison among fake image detection datasets in Tab. 1. WildFake stands out by generating a diverse array of rich, stylistically varied, and high-quality images. Within the WildFake dataset, fake images are produced either through our extensive generation pipeline or sourced from open-source communities, where users share images created with their personalized generative models. To augment the dataset’s diversity, real images are gathered from open datasets used in various tasks like image captioning, generation, and classification, ensuring a broad spectrum of styles and content. We have conducted a series of experiments on the WildFake dataset to assess the generalization capabilities of detectors trained on fake images, demonstrating WildFake’s potential in enhancing the understanding of fake image detection in a multitude of real-world scenarios. Additionally, we have implemented a series of degradation tests on the WildFake testing set, illustrating the robustness of these detectors in challenging conditions. Besides, Distinct from existing datasets, WildFake categorizes generative models into three primary groups: GANs[8, 11, 12, 36, 38–40, 69], DMs [24, 30, 32, 50, 51, 56, 59, 67], and Others [9, 10, 19, 70]. Based on these methods, WildFake uniquely features four levels of categorization, each based on different dimensions, as depicted in Fig. 1. WildFake comprehensively incorporates multiple generator types, various architectures, different model weights, and versions of the same model series. Such a structure is conducive to a detailed analysis of various image generators, offering insights of their characteristics. We plan to publicly release the WildFake dataset to support and aid the academic community.

2. Related Works

In this section, we offer a brief yet thorough exploration the image generation methods (Sec. 2.1), existing AI-generated image datasets (Sec. 2.2), and existing AI-generated image detection approaches Sec. 2.3.

2.1. Image Generation

Raging from Generative Adversarial Networks (GANs) [3, 8, 12, 19, 36, 38, 53, 63, 68, 69] to DMs (DMs) [59, 62], a multitude of users can now effortlessly produce images of high quality and diversity using varied models with personalized weights, and spread those generated images across various social media platforms. Besides, other researchers are dedicated to leveraging the autoregression models with vector quantization techniques [19, 34, 57, 70] or masked transformers [35, 45, 57] for high-quality image synthesis. We propose a tripartite classification of these generative models into: *GANs*, *DMs*, and *Others*.

GANs for Image Generation: GAN [22] was proposed to discriminate real samples from fake samples and generate more realistic samples. In the early stage, unconditional GANs: Wasserstein-GAN [5], StyleGANs [38–40], and BigGAN [8] use random vectors to generate realistic samples based on the learned distribution of training samples. Then, GANs conditioned on input single image are proposed [4, 81]. This transition led to the development of models like CycleGAN [83] and StarGAN [11, 12], which transform a given image into a desired target image through adversarial training. Recently, text-conditioned GANs, such as DF-GAN [68] and GALIP [69] were trained on pairwise text-image data and generate new images from textual descriptions. Moreover, GigaGAN [36] has introduced a novel GAN framework, showcasing the potential of GANs in the text-to-image synthesis domain.

DMs for Image Generation: DMs generators [30, 67] have recently achieved remarkable performances in image synthesis. DDPM [30] establishes a sequence of diffusion steps in a Markov chain, progressively infusing Gaussian

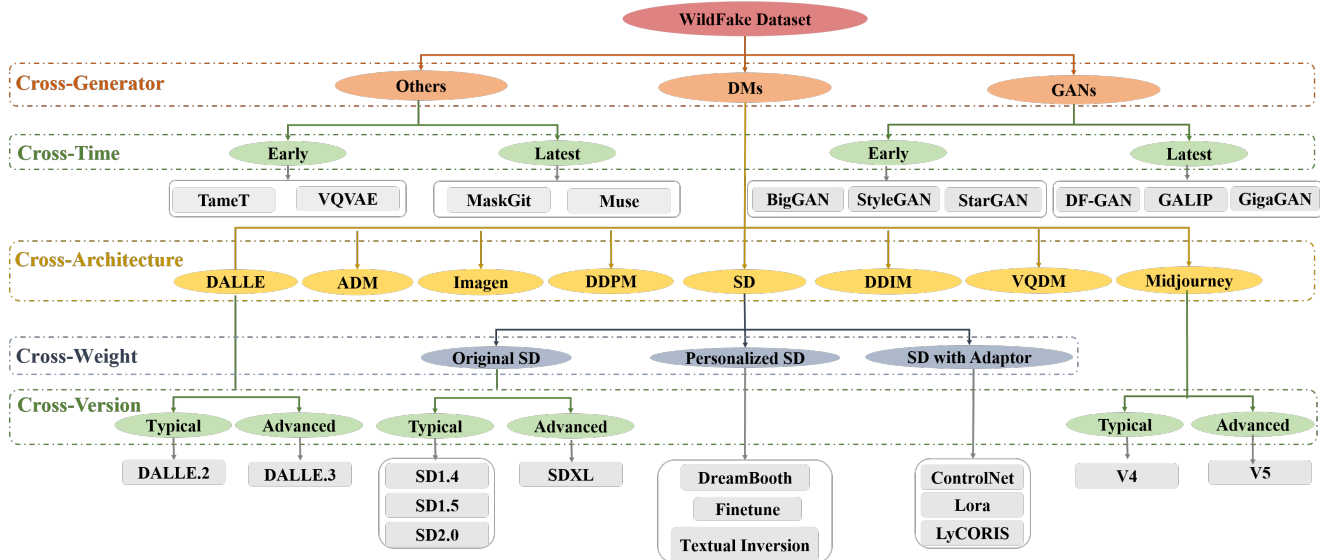


Figure 1. Overview of WildFake dataset. (a) At the cross-generator level, we separate generators into DMs, GANs, and Others. (b) The cross-architecture level discriminates different architectures from DMs, *e.g.*, DALLE [56], ADM [15], Imagen [62], DDPM [30], DDIM [67], VQDM [24], Midjourney [32], and SD [59]. Then, we separate fake images from SD [59] into three subsets according to the cross-weight level. We also introduce a cross-version level to separate different generators into typical classes and advanced classes. More the dataset details can be found in the supplementary material.

noise into the data until it converges to an isotropic Gaussian distribution in a forward process, and subsequently learns to inversely reconstruct the original data from the noise in a reverse process. DDIM [67] proposes a new deterministic method for accelerating the iterative process without the Markov hypothesis. ADM [15] finds a much more effective architecture and further achieves outstanding performance with the integration of classifier guidance. Stable Diffusion [59] (SD) is an advanced text-to-image diffusion model capable of generating highly realistic images based on any given text input. Different versions of SD including SD1.4, SD1.5, SD2.0, and SD-XL trained on large-scale datasets like Laion5B and Laion-Aesthetics dataset [2] with different dataset selection strategies to improve the quality of generated images and to ensure the safe generation of content. DALLE.2 [56] align visual embeddings to textual embeddings for supporting text-to-image generation and image-to-image generation, and DALLE.3 [51] adopt advanced caption system to improve the quality of training image-text pairs. VQDM [24] proposes a latent-space method that eliminates the unidirectional bias with previous methods and incorporates a mask-and-replace diffusion mechanism to alleviate the accumulation of errors. Imagen [62] adopt a generic large language model pre-trained on text-only corpora to generate high-fidelity images. Beyond these academic contributions, Midjourney [32] is one of the most renowned commercial software programs, known for its exceptional image gener-

ation performance. Our implementation employs Midjourney V5 for image generation, which offers more intricate details compared to previous versions, yielding images that closely resemble real-world photographs.

Other Image Generation Approaches: In addition to DMs and GANs, other generative models also demonstrate potential for high-quality image synthesis and offer valuable insights for theoretical analysis. These include Variational Auto-Encoders (VAEs) [17, 29, 43] and Flow-Based Models [16, 42, 58]. Recent developments have further demonstrated the capability of other type of generative models in producing high-quality images. VQVAE [70] introduce vector quantization technique into VAEs [6] to solve vague problems in VAEs. Vector quantization [70] is also combined with autoregression model in TameT [19] to produce high-resolution images. Masked Generative Encoder [27, 45] represents a convergence of masked generative models and self-supervised representation learning. This union forms a robust framework for image synthesis, leveraging the strengths of both paradigms to enhance the generative process. MaskGit [9] introduces a bidirectional transformer decoder. This innovative mechanism enables simultaneous token generation for an entire image, which is then progressively refined in an iterative manner, predicated on the tokens generated in the preceding iteration. Muse [10], a text-to-image Transformer model, is also noteworthy. It is trained on a masked modeling task in discrete token space, utilizing text embeddings extracted from a pre-

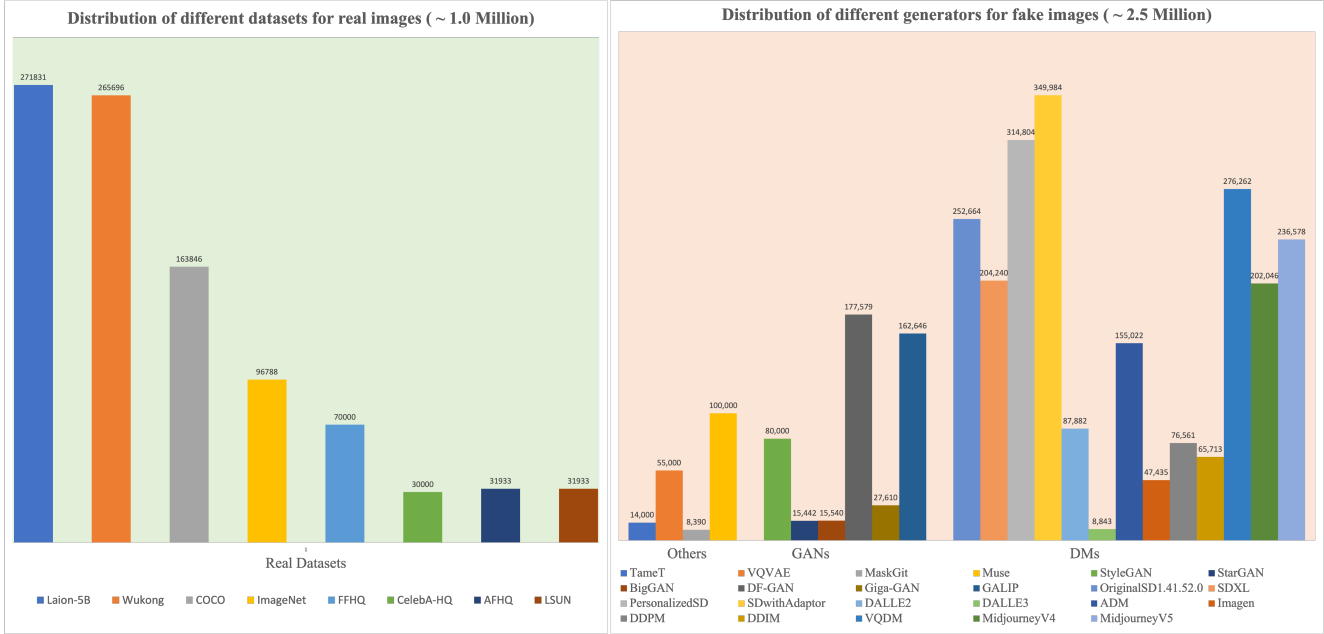


Figure 2. Overview of data distribution of WildFake dataset. The left subfigure shows the distribution of real images from open-source datasets, and the right subfigure represents fake images sourced from different generators.

trained large language model to achieve impressive image generation performance.

2.2. AI-Generated Image Datasets

To enhance the development of AI-generated image detectors, early datasets primarily utilized GANs. For instance, CNNSpot [74] builds its foundation on GAN-generated images. This dataset exclusively uses ProGAN [37] to generate its training set and assesses the performance of detectors across various GAN-based testing sets. However, the recent advent of alternative generators besides GANs, such as DMs, has significantly improved the quality of generated images. This advancement complicates the differentiation between real and synthetic images. Consequently, investigating images produced by DMs becomes crucial. In response to this need, IEEE VIP Cup [71] and DE-FAKE [66] have incorporated DMs to create more diverse images, using prompts from the MSCOCO dataset [46] and Flickr30k dataset [79]. Based on a small-scale Cifar10 dataset [44], CiFAKE [7] generates fake images only with Stable Diffusion V1.4 [59]. DiffusionDB [76], constructed by collecting images shared on the Stable Diffusion public Discord server [31], does not categorize DiffusionDB dataset based on different dimensions like model architectures and parameters. This lack of differentiation hinders the evaluation of detectors using multi-dimensional metrics. Artifact [55] generates fake images using real prompts from existing datasets. However, this approach limits the diversity

and creativity of the fake images, as they are constrained by the originality of the prompts. GenImage [84] also faces limitations, relying on the 1000 classes from ImageNet dataset [61] to produce limited content. It is not suited to real-world scenarios where users create fake images using a variety of random textual information. DiffusionForensics dataset is proposed in DIRE [75] which adopt several DMs to produce fake images based on LSUN-Bedroom [80], ImageNet [61], and CelebA-HQ [37] dataset.

Current datasets in this field tend to focus on a limited range of image generators, resulting in a narrow representation of fake images. These datasets often feature synthetic images either created by the developers themselves or sourced from a handful of open-source platforms, thus offering a restricted view of the diversity and intricacy inherent in fake imagery. In contrast, our study adopts a broader approach, systematically collecting and generating fake images from various open-source websites and diverse generators according to a hierarchical construction structure. This method offers a more comprehensive perspective on the complexity of AI-Generated Image Detection.

2.3. AI-Generated Image Detectors

A naive method is to establish a classification model to distinguish fake images from real images via finetuning pre-trained discriminative models such as ViT [52] or ResNet [26] for fake vs. real image classification. DIRE [75] is mainly designed to distinguish images gen-

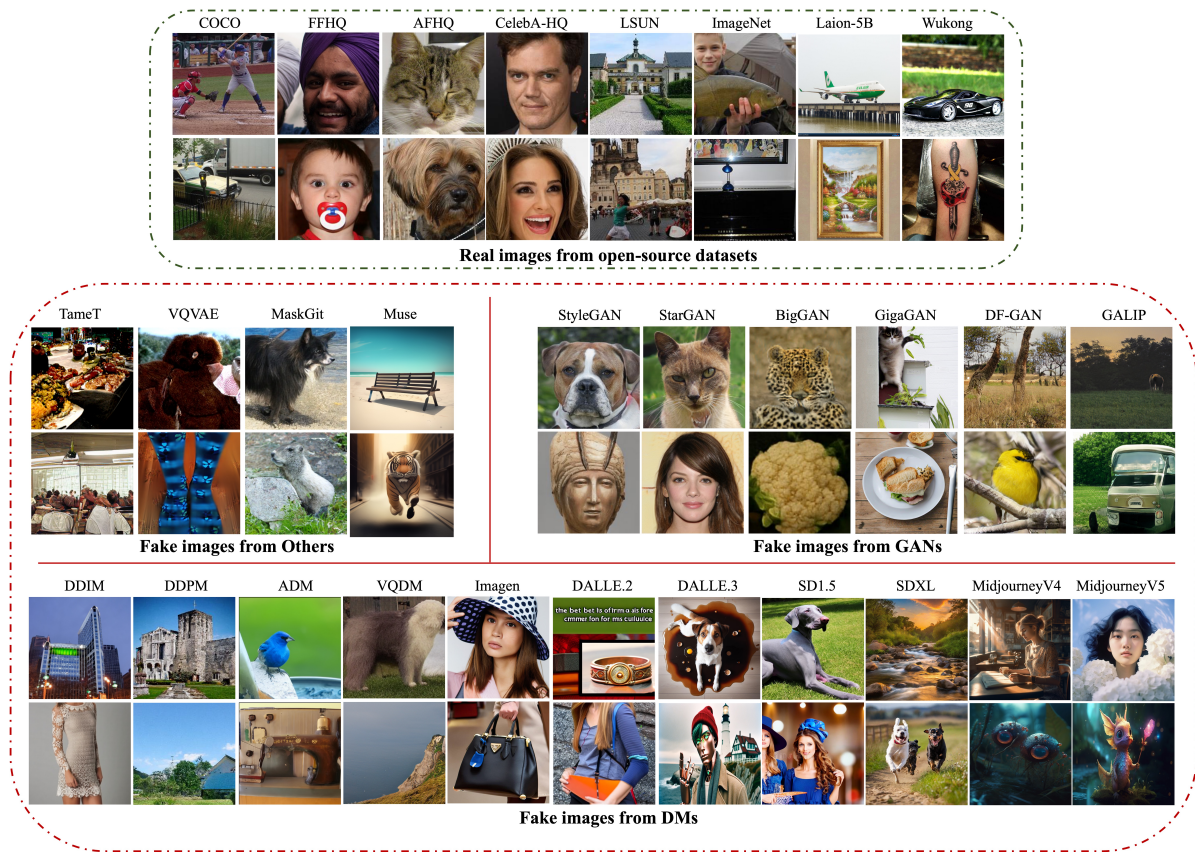


Figure 3. Visualization of some real images and fake images from the WildFake dataset.

erated by DMs models from real images by measuring the error between an input image and its reconstruction counterpart by a pre-trained diffusion model. IFDL [25] introduces a multi-branch system combining feature extraction, localization, and classification to assign multi-level labels to fake images. multiLID [47] employs feature-map representations of fake images and calculates multi-local intrinsic dimensionality for classifier training. LASTED [77] formulates synthetic image detection as an identification problem by augmenting the training images with carefully designed textual labels with joint image-text contrastive learning.

3. Dataset Construction

Addressing the critical need for assessing the generalizability and robustness of fake image detectors, we have developed the “WildFake” dataset, which meets two principal criteria:

- **Diverse Content with Wild Collection:** WildFake includes a wide array of high-quality fake images sourced from open-source websites, along with images produced using both user-trained and officially provided pre-trained generative models. This diverse collection ensures a com-

prehensive set of fake images, significantly enriching the understanding of fake image detection across numerous real-world contexts.

- **Hierarchical Structure:** The dataset is organized hierarchically, encompassing cross-generators, cross-architectures within the same type of generator, cross-weights within identical architectures, and cross-time analysis either within the same generator type or across different versions of the same model series. This structure facilitates in-depth analysis of various image generators.

3.1. Organization of WildFake Dataset

As is shown in Fig. 1, the proposed WildFake dataset consists of five levels consisting of *cross-generator*, *cross-architecture*, *cross-weight*, *cross-time*, and *cross-version*.

- **Cross-Generator:** This level encompasses DMs, GANs, and Other generators, providing a comprehensive overview of the diverse generative models in use.
- **Cross-Time:** Focusing on GANs and Other generators known for high-quality synthesis, we categorize them into “Early” and “Latest” groups. “Early” represents well-established, popular models, whereas “Latest” includes

recent advancements. Early GANs (*advanced GANs*) consists of BigGAN [8], StyleGANs [38–40], and StarGANs [11, 12], (*resp.*, GigaGAN [36], DF-GAN [68], and GALIP [69]). Similarly, for Others generators, “Early” includes VQVAE [70] and VQGAN [19], while “Latest” encompasses Muse [10] and Maskgit [9].

- **Cross-Architecture:** Considering the rapid development of DMs generators, nine kinds of DMs generators comprise cross-architecture level, consisting DALLE [56], ADM [15], Imagen [62], DDPM [30], DDIM [67], VQDM [24], Midjourney [32], and SD [59].
- **Cross-Weight:** Open-source SD [59] has been widely spread in academia and industry, officially released pre-trained models armed with updated architecture trained on large datasets, and users also adopt different finetuning strategies such as finetuning several modules of SD [59] or finetuning with DreamBooth [60] to obtain personalized models. Besides, many works focus on training different adaptors to combine with the base SD model to achieve controllable generation. ControlNet [82] relies on paired image-prior data to control different prior information of generated images like edge, segmentation mask, style, and etc. Lora-based methods including Lora [33] and LyCORIS [78] are also proposed to train extra low-rank layers to incorporate new content into the base model. Also, there are some methods [21, 72] to learn new tokens on the user-provided data for customized image generation. Thus, we classify SD-based generators into Original SD, Personalized SD, and SD with adaptors for cross-weight evaluation.
- **Cross-Version:** DALLE [56], Midjourney [32], Imagen [62], and SD [59] have been widely known in academia and industry, due to the superiority of the quality of generated images. Fake images in DALLE [56] (*resp.*, Midjourney [32]) are divided into “Typical” and “Advanced” subsets along the cross-version level.

3.2. Image Collection

Fake Image Collection: To collect diverse fake images from different resources, we have established a generation pipeline. This pipeline facilitates the production of images using popular generative mechanisms, including GANs, DMs, and Others generators. Besides, we sourced user-created images from open-source platforms such as Civitai [28] and Midjourney [32]. On these platforms, users generate new images using either original open-source models or personalized models fine-tuned with their data. Unlike datasets primarily composed of author-generated images, such as DiffusionForensics [75], ArtiFact [55], and GenImage [84], our approach of collecting from open sources offers a more representative sample of the average quality of generated images. This ensures that the evaluation of detection models on our dataset is reflective of

real-world applicability. For gathering images from GANs and Others, we primarily utilize official GitHub repositories and model cards from Hugging Face. When these GitHub repositories include generated samples, we directly extract fake images from there. In cases where the methods are associated with text-to-image generation, new images are produced by randomly sampling captions from their respective testing datasets. For other scenarios, we randomly generate images using the pretrained models available.

Real Image Collection: Considering the fact that some fake images from GANs and Others are limited to specific domains determined by training datasets such as COCO [46], FFHQ [38], ImageNet [14], LSUN Church [80], CelebA-HQ [37], AFHQ [12] dataset, we sample parts of real images from those datasets. Besides, recent text-to-image generators mostly trained on Laion-5B [65] or Chinese cross-modal Wukong [23] datasets, we also include real image samples from these text-to-image datasets. This ensures a comprehensive collection of real images, facilitating a more robust and realistic evaluation of image authenticity.

3.3. Analyses of WildFake

Examples of images from WildFake’s various categories are displayed in Fig. 3. To analyze WildFake, we illustrate the distribution of both real and fake images from various sources in Fig. 2 for fake images and Fig. 2 for real images. The WildFake dataset contains a total of 3,694,313 images, comprising 1,013,446 real images and 2,680,867 fake images. We split real images (*resp.*, fake images) into the training set and testing set as the ratio of 4 : 1. In detail, for all generators in Fig. 2, 20% samples are randomly selected as the testing set from fake images generated by each generator, with the remainder forming the training set. A similar splitting strategy is applied to the real datasets shown in Fig. 2.

4. Experiments

In this section, we conduct comprehensive experiments on WildFake to evaluate state-of-the-art AI-generated image datasets/detectors from multi-dimensional aspects. We also compare the generalization of detectors trained on different datasets. First, we evaluate the generalization ability of the trained detectors, including cross-generator evaluation, cross-architecture evaluation, cross-weight evaluation, and cross-time evaluation in Appendix D. Second, we focus on evaluating the robustness of the trained detectors by imitating propagation degradation problems in Sec. 4.4.

4.1. Experimental Settings

Baselines. We select high-quality and large scale AI-generated image datasets (see Sec. 2.2 and Tab. 1) as baseline datasets, including *DiffusionDB* [76], *ArtiFact* [55],

Table 2. Evaluating the superiority of our proposed WildFake dataset. ResNet50-ArtiFact (*resp.*, ResNet50-WildFake) denotes the detector with ResNet50 architecture trained on ArtiFact (*resp.*, WildFake dataset). ViT-ArtiFact (*resp.*, ViT-WildFake) denotes the detector with ViT architecture trained on ArtiFact, dataset (*resp.*, WildFake dataset). (ACC(%), AP(%), and AUC(%)) are reported.

Training Detectors and Datasets	Testing Dataset					Avg
	DiffusionForensics	GenImage	DiffusionDB	ArtiFact	WildFake	
ResNet50-ArtiFact	85.4/94.9/76.7	76.5/84.8/82.9	64.1/69.9/68.1	97.2/99.5/99.3	85.4/94.9/76.7	81.7/88.8/80.74
ResNet50-WildFake	87.2/96.6/83.4	80.9/89.9/89.3	96.3/99.2/ 99.2	68.0/84.7/75.3	99.6/99.9/99.9	86.4/94.1/89.42
ViT-ArtiFact	84.2/96.1/82.5	78.5/88.1/85.0	68.4/75.3/73.2	96.8/99.6/99.5	84.2/96.1/82.5	82.4/91.0/84.4
ViT-WildFake	95.8/99.1/97.2	88.6/83.6/89.7	99.3/99.8/99.9	62.2/81.9/68.8	99.1/99.9/99.9	89.0/92.84/91.1

Table 3. Results of cross-generator evaluation on different training and testing subsets using ViT.

Training Subset	Testing Subset		
	DMs	GANs	Others
DMs	99.7/99.9/99.9	86.4/95.9/89.8	79.3/93.5/84.5
GANs	77.1/83.2/74.3	98.1/99.0/99.6	91.4/97.2/94.6
Others	76.4/77.2/70.1	82.5/96.0/91.2	99.6/99.9/99.9

GenImage [84], and *DiffusionForensics* [75]. Each of these datasets follows their original train-test split strategies. The baseline detectors selected for evaluation in our study include *DIRE* [75], *IFDL* [25], *multiLID* [47], *LASTED* [77], *ViT* [18] and *ResNet50* [26]. For detailed descriptions of these detectors, please refer to Sec. 2.3. For baseline methods, we follow the experimental setting from original paper. For naive methods, ResNet50 (*resp.*, ViT) is pretrained on ImageNet datasets (*resp.*, LAION-5B). All training images are resize to 224×224 , with the Adam optimizer and Exponentially Decay scheduler with an initial learning rate of $1e - 4$, and batch size (*resp.*, epoch) is set as 1024 (*resp.*, 15).

Evaluation Metrics. Following previous AI-generated image detection methods [73, 74], we report accuracy (ACC) and average precision (AP) in our experiments to evaluate the detectors. The threshold for computing accuracy is set to 0.5 following [74]. Besides, we include the Area Under the ROC Curve (AUC) as another critical metric.

4.2. Superiority of WildFake to Baselines

Considering the rich and diverse content of WildFake, including wild, diverse, and hierarchical-quality fake images generated by GANs generators, DMs generators, and Others generators, detectors trained on WildFake can achieve better performance compared with other existing baseline datasets. For a comparative analysis, we have chosen the ArtiFact [55] dataset as a baseline, considering its volume and diversity. We train detectors using the basic ResNet50 [26] (*resp.*, ViT [54]) on ArtiFact [55] and WildFake. Then, evaluate the both trained detectors on the testing set of all baseline datasets and WildFake. The comparison results are reported in Tab. 2, we can see that de-

tor ResNet50-WildFake (*resp.*, ViT-WildFake) outperform ResNet50-ArtiFact (*resp.*, ViT-ArtiFact) over DiffusionForensics, DiffusionDB, and GenImage datasets. This is especially evident for DMs-centric datasets like DiffusionForensics and DiffusionDB. More comparison experiments on WildFake using different detectors are provided in Supplementary.

4.3. Generalization Capability Evaluation

Owing to the hierarchical structure of WildFake, the trained detectors’ generalization capabilities can be evaluated across various hierarchical dimensions, a feature that is not applicable to other baseline datasets. As depicted in Fig. 1, WildFake is systematically divided into five distinct levels: the first level is cross-generators consisting of three types of generators, the second level is cross-architecture in DMs generators consisting of eight types of DMs architectures, the third level is the cross-weight in SD consisting of three types of weights, the last two levels are cross-version and cross-time in three types of generators consisting of typical (*resp.*, early) generators and advanced (*resp.*, latest) generators. We utilize the baseline detector ViT to conduct comprehensive generalization experiments: (1) Cross-generator experimental comparison is designed to evaluate the gap among different generators in Tab. 3. (2) Comparison among cross architectures is designed to evaluate the effects of DMs generators with different architectures in Tab. 4. (3) Cross-weight evaluation of SD, cross-time evaluation of GANs (*resp.*, Others), and cross-version evaluation of Midjourney (*resp.*, SD) are reported in Supplementary due to space limit.

Evaluation on Cross-Generator. We first assess the performance of the ViT detector when trained and tested on images generated by the same type of generator within WildFake. Our WildFake dataset consists of three types of generators including DMs, GANs, and Others. Accordingly, we divide the WildFake dataset into three subsets, each with its training and testing set, based on the generator type. We then train the ViT model separately on each generator type and evaluate its performance on the corresponding testing set of each type. The results in Tab. 3 indicate that the in-domain generalization ability is significantly superior to

Table 4. Results of cross-architecture from DMs generator on different training and testing subsets using ViT.

Training Subset	Testing Subset							
	ADM	DALLE	DDIM	DDPM	Imagen	VQDM	Midjourney	SD
ADM	100/100/100	93.3/98.9/97.8	78.6/90.9/84.0	80.5/92.0/86.1	96.9/99.3/99.0	90.6/97.6/96.0	84.4/92.8/89.3	87.6/97.0/94.1
DALLE	90.0/91.8/90.6	99.9/99.9/99.9	99.7/99.9/99.9	98.3/99.8/99.7	99.9/99.9/99.9	79.0/77.7/71.1	80.4/78.8/72.3	85.7/89.7/86.9
DDIM	89.9/91.0/87.1	99.7/99.9/99.9	99.9/99.9/99.9	99.7/99.9/99.9	99.9/99.9/99.9	75.6/79.9/71.0	76.2/85.5/78.0	88.5/90.7/86.1
DDPM	92.0/89.9/88.5	99.7/99.9/99.8	99.9/99.9/99.9	99.8/99.9/99.9	100/100/100	76.0/74.1/64.9	77.0/75.7/67.8	89.1/88.7/86.1
Imagen	80.3/92.4/85.2	98.6/99.7/99.3	95.0/98.5/97.1	94.7/98.3/96.4	100/100/100	81.8/89.1/85.4	84.0/89.8/86.9	77.3/91.3/82.7
VQDM	91.8/98.1/96.7	88.4/96.5/91.3	79.7/85.4/79.6	71.0/84.0/67.1	98.1/99.4/98.6	99.9/99.9/99.9	95.7/98.7/97.4	93.5/98.0/95.8
Midjourney	99.9/99.9/99.9	99.9/99.9/99.9	99.6/99.9/99.9	99.4/99.9/99.9	100/100/100	99.9/99.9/99.9	99.9/99.9/99.9	99.8/99.9/99.9
SD	99.9/99.0/99.9	100/100/100	99.7/99.9/99.9	99.3/99.9/99.9	100/100/100	99.9/99.9/100	99.9/100/99.9	100/99.9/100

Table 5. Robustness evaluation of different detectors trained on the proposed WildFake dataset. “Trans” denotes Transformation.

Method	DownSample		Compression		Geometric Transformation		Watermarks		Color Trans
	128	64	q=70	q=35	Flip	Crop	Text	Image	
ResNet50	91.1/95.5/93.1	71.3/65.0/39.8	84.6/95.9/92.5	85/93.1/87.7	95.1/98.4/96.4	91.3/98.7/96.9	91.0/98.8/94.1	90.8/98.8/93.9	87.9/97.3/94.8
ViT	91.8/94.6/92.4	79.3/78.2/66.2	92.4/98.1/96.0	86.6/95.1/95	97.1/99.8/99.4	98.9/99.9/99.1	93.6/99.3/96.6	92.9/99.3/96.5	98.5/99.9/99.8

cross-domain generalization. Notably, models trained on DMs exhibit a lesser degree of generalization compared to those trained on GANs and Others. This suggests that the disparity between DMs and GANs (*resp.*, Others) is more pronounced than that between GANs and Others. We hypothesize that this is due to the distinct image generation approaches: while Others and GANs typically employ one-step inference for image generation, DMs utilize multiple denoising steps.

Evaluation on Cross-Architecture of DMs Considering the high quality of images generated by DMs, we further classify images from DMs into 8 categories according to the difference of architectures consisting of SD, DDPM, DDIM, ADM, DALLE, Imagen, Midjourney, and VQDM. The performance of detectors over cross-architecture scenarios is observed to be worse to that of in-architecture validations. This suggests that different architectures within DMs generators might produce fake images with varying levels of sophistication. Another notable finding is that models trained on Midjourney and SD demonstrate superior generalization ability compared to other architectures. The reasons for this are threefold: (1) The volume of training images from Midjourney and SD is greater than that of other architectures, offering a more extensive learning base. (2) The content diversity of fake images from Midjourney and SD is richer, providing a broader spectrum of data for model training. (3) A portion of the fake images in Midjourney and SD are sourced from open community platforms, typically exhibiting higher quality compared to those from other architectures.

4.4. Robustness to Degraded Images

Images often suffer from degradation problems during propagation [64], such as low resolution, noise interference, and watermarks. It is crucial for detectors to demonstrate

resilience against these challenges. To assess the robustness of detectors trained on the WildFake dataset in handling degraded images, we implement a series of degradation techniques on the testing set images: (1) DownSample: down-sampling the high-resolution images to resolutions of 128 or 64. (2) Compression: introducing compression artifacts to the testing set by applying JPEG compression with quality ratios on the original test images. (3) Geometric Transformation: Randomly flipping or cropping the images from the testing set. (4) Watermark: randomly adding textual or visual watermarks on the random position of images from the testing set. (5) Color Transformation: we randomly change the brightness, contrast, saturation, and hue of images from the testing set. We report the robustness results of ResNet50-WildFake and ViT-WildFake over those degraded testing images in Tab. 5. Other baseline methods evaluated with this degradation settings on WildFake are provided in Supplementary. Analysis of the results reveals that the ViT-based detector exhibits superior performance on these degraded images compared to the ResNet-50-based detector. The ResNet-50-based detector shows greater sensitivity to geometric and color transformations, whereas the ViT-based detector demonstrates better robustness. Both detectors experience a decline in performance when confronted with image-based or text-based watermarks. It is also observed that lower resolutions (*resp.*, low quality) significantly affect the accuracy of the trained detectors.

5. Conclusion

In this paper, we present a large-scale dataset WildFake, to assess the generalizability and robustness of fake image detection. WildFake amasses a diverse array of fake images from the open-source community, featuring a wide range of image classes and styles. The dataset includes fake images generated by various types of generators, encompass-

ing GANs, diffusion models, and other generative models. The key strengths of WildFake notably enhance the generalization and robustness of detectors trained with this dataset, showcasing its significant applicability and effectiveness in real-world scenarios for AI-generated image detection. Furthermore, our in-depth evaluation experiments are designed to provide substantial insights into the capabilities of generative models at different levels, a unique benefit derived from WildFake’s distinct hierarchical structure.

Appendix

In this supplementary material, we provide detailed information and additional analyses that complements our main submission. The sections are structured as follows: In Appendix A, we provide a comprehensive overview of the baseline datasets and detectors utilized in our study, providing a foundation for understanding the experimental setup and detector methodologies. In Appendix B, we present more cross-dataset validation comparisons. This section aims to underscore the advancements and superiority of our proposed WildFake dataset in comparison to existing benchmarks. In Appendix C, we systematically compare the performance of various baseline detectors across different datasets. This comparative analysis is pivotal in evaluating the effectiveness and adaptability of each detector. In Appendix D, we present cross-weight, cross-time, and cross-version evaluations. It offers an in-depth analysis of the proposed WildFake dataset, highlighting its robustness and versatility in various scenarios. Finally, in Appendix E, we examine and compare the robustness of different detectors when trained on the proposed WildFake dataset, aiming to showcase the resilience of these detectors against various challenges and degradation scenarios.

A. Experimental Details

Baseline Detectors.

- *DIRE* [75] is specifically designed to differentiate between images generated by DMs and real images. It achieves this by measuring the discrepancy between an input image and its reconstructed counterpart using a pre-trained DM. In accordance with the original setup of DIRE [75], we utilize the ADM network[15], pre-trained on the LSUN-Bedroom dataset [80], as the reconstruction model. This model is employed to calculate reconstructed images for each input. For obtaining these reconstructed images, we adopt the DDIM [67] inversion and reconstruction process, with the number of diffusion steps set to 20 by default. A ResNet-50 model [26] is used as the classifier in this framework.
- *IFDL* [25] leverages multi-branch feature extractor, along with localization and classification modules, designed to represent the attributes of a fake image with multiple la-

bels at different levels. In line with the original setup in IFDL [25], the IFDL model is trained for 400,000 iterations with a batch size of 16, evenly split between 8 real and 8 fake images. Given that images in our WildFake dataset are categorized into five-level subsets, including cross-generator, cross-architecture, cross-weight, cross-version, and cross-time, we have adapted the IFDL [25] method accordingly. This adaptation involves a modification based on these five levels, setting all masks to 0, as our current focus is solely on fully-synthesized images.

- *Multi-LID* [47] focuses on extracting feature-map representations of fake images and calculating multi-local intrinsic dimensionality to train a classifier. Following the settings in Multi-LID [47], the process begins by calculating the standard mean and deviation across the dataset to normalize the inputs, ensuring a uniform data distribution. Then, images are processed through an untrained ResNet18 model[26] to extract their features, which are then utilized to compute Multi-LID scores. The experimental setup includes a training dataset comprising 1,600 samples per class. Finally, a random forest classifier is trained using the labeled Multi-LID scores to discern between real and fake images.
- *LASTED* [77] treats synthetic image detection as an identification problem, enhancing training images with meticulously designed textual labels for joint image-text contrastive learning. The implementation of LASTED [77] employs the Adam optimizer [41], with an initial learning rate set at $1e - 4$. The learning rate is halved if validation accuracy does not improve for two consecutive epochs, continuing until convergence is achieved. During the training and testing phases, all input images are randomly or center cropped into 448×448 patches. Image augmentation techniques, such as compression, blurring, and scaling, are applied with a 50% probability. The batch size for the process is set at 48. The batch size is set to 48. Given that images from the WildFake dataset and other baseline datasets do not come with specific style labels, we adhere to the \mathcal{R}_1 setting in LASTED [77]. Here, textual labels are defined simply as “Real, Synthetic” during the training stage.
- *Naive methods* utilize pre-trained discriminative models, specifically *ViT*[18] and *ResNet50*[26], to differentiate between generated and real images. For this purpose, the ResNet50 model (*resp.*, ViT) is pre-trained on the ImageNet datasets (*resp.*, LAION-5B). All training images are resized to 224×224 pixels. We employ the Adam optimizer alongside an Exponentially Decay scheduler for learning rate adjustment, starting with an initial rate of $1e - 4$. The batch size is set at 1024, with the training process lasting 15 epochs.

Baseline Datasets

- *DiffusionDB* [76] assembles images that have been shared

Table 6. Cross-dataset generalization results of DIRE detector trained on different datasets.

Training Dataset	Testing Dataset					Avg
	DiffusionForensics	GenImage	DiffusionDB	ArtiFact	WildFake	
GenImage	82.9/93.9/76.7	99.5/99.9/99.9	91.3/94.5/92.5	59.1/61.8/52.7	72.1/92.3/80.4	80.9/88.4/80.4
DiffusionDB	82.7/82.7/53.4	50.0/49.3/47.1	99.9/99.9/99.9	60.3/60.3/50.1	79.1/81.0/72.0	74.4/74.6/64.5
ArtiFact	79.5/88.3/74.6	75.4/82.0/82.3	59.9/64.8/62.5	92.4/92.6/92.4	69.8/83.4/70.2	75.4/82.2/76.4
WildFake	85.5/97.5/84.9	77.3/85.1/84.5	97.2/99.3/99.3	67.6/84.0/74.8	89.3/89.6/89.7	83.4/91.1/86.6

Table 7. Cross-dataset generalization results of IFDL detector trained on different datasets.

Training Dataset	Testing Dataset					Avg
	DiffusionForensics	GenImage	DiffusionDB	ArtiFact	WildFake	
GenImage	86.4/95.9/81.4	99.6/99.9/99.9	93.7/96.8/95.0	61.4/67.4/55.1	74.2/93.7/83.9	83.0/90.7/83.0
DiffusionDB	88.3/88.1/53.9	52.9/51.8/51.0	99.9/100/100	63.4/62.4/53.5	85.5/85.9/76.5	78.0/77.6/66.9
ArtiFact	87.9/95.8/80.0	78.3/87.1/84.9	66.2/72.1/69.1	97.6/99.6/99.6	71.9/90.0/75.5	80.3/88.9/81.8
WildFake	88.6/97.9/92.8	85.1/95.0/89.9	97.7/99.5/99.7	67.7/82.1/72.4	99.3/99.9/99.9	87.6/93.9/99.0

on the Stable Diffusion public Discord server [31].

- *ArtiFact* [55] generates fake images using real prompts sourced from actual datasets. In total, the dataset comprises 2,496,738 images, of which 964,989 are real and 1,531,749 are fake. The dataset predominantly features categories such as Human/Human Faces, Animal/Animal Faces, Vehicles, Places, and Art. It utilizes 13 GANs and 7 DMs for image generation. Notably, the number of fake images produced by GANs significantly exceeds those generated by DMs.
- *GenImage* [84] primarily utilizes the 1000 classes from the ImageNet dataset [61] to generate its content. It contains over one million pairs of real and fake images, fully incorporates all the real images available in ImageNet. For image generation, *GenImage* leverages the 1000 distinct labels present in ImageNet. In total, the dataset consists of 2,681,167 images, divided into 1,331,167 real and 1,350,000 fake images. Of the real images, 1,281,167 are allocated for training purposes, and 50,000 are set aside for testing.
- *DiffusionForensics* [75] utilizes a variety of DMs to create fake images. These images are based on several well-known datasets: LSUN-Bedroom [80], ImageNet [61], and CelebA-HQ [37]. Each of these source datasets is divided into training and testing sets, adhering to their respective original split strategies. In total, the DiffusionForensics dataset comprises 439,020 fake images generated by DMs, alongside 92,000 real images.
- *WildFake* contains a total of 3,694,313 images, of which 1,013,446 are real and 2,680,867 are fake. We have divided both real and fake images into training and testing sets, maintaining a ratio of 4 : 1 for each category. Specifically, for every generator used in the dataset, 20% of the fake images they produce are randomly selected

to constitute the testing set, while the remaining 80% are allocated to the training set. This systematic approach ensures a balanced and representative distribution of images for both training and evaluation purposes.

B. Demonstrating WildFake’s Superiority over Baseline Datasets.

The WildFake dataset stands out due to its rich and diverse content. It contains a wide array of fake images characterized by their wild, varied, and hierarchically-structured quality, produced by an assortment of generators, including GANs, DMs, and Others. This diversity and depth in content enable detectors trained on the WildFake dataset to achieve superior performance when compared to those trained on other existing baseline datasets. The varied nature of the images within WildFake provides a more comprehensive training ground, thereby enhancing the detectors’ ability to generalize and adapt to a broader range of synthetic images. In this section, we select *GenImage* [84], *DiffusionDB* [76], and *ArtiFact* [55] as comparable datasets for our analysis. We train the same set of detectors on these baseline datasets as well as the proposed WildFake dataset. This setup allows us to conduct cross-dataset experiments aimed at evaluating the cross-dataset generalization capabilities of detectors trained on various datasets. For this cross-data generalization validation, we employ a range of baseline detectors including DIRE [75], IFDL [25], Multi-LID [47], LASTED [77], ResNet50 [26], and ViT[18] as baseline detectors to implement cross-dataset comparison. The cross-data generalization comparison results from DIRE [75] (*resp.*, IFDL [25], Multi-LID [47], LASTED [77], ResNet50 [26], and ViT[18]) are reported in Tab. 6 (*resp.*, Tab. 7, Tab. 8, Tab. 9, Tab. 10, and Tab. 11). The comparison results demonstrate that baseline

Table 8. Cross-dataset generalization results of Multi-LID detector trained on different datasets.

Training Dataset	Testing Dataset					Avg
	DiffusionForensics	GenImage	DiffusionDB	ArtiFact	WildFake	
GenImage	58.8/59.9/51.5	75.8/73.9/74.9	59.1/60.4/52.0	49.9/45.3/42.9	50.5/61.5/54.3	58.8/60.2/55.1
DiffusionDB	50.0/50.8/45.6	47.0/46.5/44.9	77.2/72.4/73.4	49.9/51.9/49.0	51.0/49.4/48.9	55.0/54.2/52.3
ArtiFact	55.7/61.4/54.7	53.6/59.6/58.4	49.9/50.9/49.7	71.0/72.7/73.5	50.8/59.7/51.9	56.2/60.9/57.4
WildFake	56.7/58.8/54.4	52.1/58.2/58.1	62.1/64.5/64.6	51.2/55.1/56.0	74.3/75.9/75.9	59.2/62.5/61.8

Table 9. Cross-dataset generalization results of LASTED detector trained on different datasets.

Training Dataset	Testing Dataset					Avg
	DiffusionForensics	GenImage	DiffusionDB	ArtiFact	WildFake	
GenImage	87.6/96.2/83.7	99.8/99.9/99.9	94.3/97.9/95.7	63.4/66.7/57.0	78.8/94.3/86.9	84.7/91.0/84.6
DiffusionDB	90.7/90.5/58.4	53.1/53.2/52.3	99.9/100/100	65.4/66.5/55.9	88.2/90.0/79.1	79.4/80.0/69.1
ArtiFact	91.3/98.6/84.1	80.2/89.1/89.2	69.5/75.7/72.6	98.2/99.7/99.6	73.0/92.0/77.8	82.4/91.1/84.7
WildFake	94.9/98.1/96.2	87.0/91.4/93.8	98.9/99.7/99.8	71.4/89.0/79.1	99.7/99.9/99.9	93.0/95.6/93.7

detectors trained on the proposed WildFake dataset exhibit the best cross-dataset generalization ability. This suggests that the diverse and high-quality content of the WildFake dataset, primarily sourced from open-source websites, plays a crucial role in training detectors with a high degree of generalization to various datasets. The inclusion of a hierarchical structure in WildFake further contributes to this by covering different generalization methods and ensuring a comprehensive dataset. Another noteworthy observation is that detectors trained on the GenImage [84] or ArtiFact [55] datasets show better generalization performance compared to those trained on the DiffusionDB [76] dataset. This can be attributed to the fact that DiffusionDB primarily collects fake images generated by diffusion-based generators using the 1000 category labels from the ImageNet dataset. Such a focused collection results in a dataset with limited diversity, which may constrain the generalization ability of the trained detectors.

C. Comparison of Baseline Detectors

In this section, we analyze and compare the cross-dataset generalization performance of various baseline detectors trained on the same dataset. The baseline detectors included in our analysis are DIRE [75], IFDL [25], Multi-LID [47], LASTED [77], ResNet50 [26], and ViT [18]. The cross-dataset generalization comparison results of different baseline detectors trained on GenImage [84] (*resp.*, DiffusionDB [76], ArtiFact [55], and WildFake) dataset are reported in Tab. 12 (*resp.*, Tab. 13, Tab. 14, and Tab. 15). In our comparative analysis, LASTED [77] emerges as the top performer in terms of generalization across GenImage [84], DiffusionDB [76], ArtiFact [55], and WildFake. The results notably indicate that LASTED’s use of language guidance significantly enhances its generalizability across different

datasets. Another key observation is that IFDL [25] also achieves comparable performance, which can be attributed to its multi-branch feature extractor that is adept at learning fine-grained features. In contrast, DIRE [75], while specifically designed for detecting diffusion-based fake images via a reconstruction method, shows limited generalization to other datasets. This limitation may stem from its focus on a specific type of generator and neglecting the variations among different generators. Additionally, we observe that the naive methods, including ResNet50 [26] and ViT [18], also perform satisfactorily across these datasets. This can be explained by the fact that training with large-scale datasets, encompassing more than one million images, facilitates the development of a data-driven classifier adept at AI-generated image detection.

D. Generalization Evaluation

Leveraging the diverse and comprehensive nature of WildFake, we have developed a series of comparative experiments to assess the generalization capabilities of various detectors. Recognizing the popularity of Stable Diffusion, which includes numerous personalized and finetuned models as well as target-oriented adaptors, we have designed cross-weight comparison experiments. These experiments, detailed in Tab. 16, aim to evaluate the generalization ability across different weights within Stable Diffusion. For the three types of generators (Stable Diffusion, GANs, and Others), we perform evaluations that focus on both cross-time and cross-version aspects. This involves training detectors on Typical/Early (*resp.*, Advanced/Latest) models and then testing on Advanced/Latest (*resp.*, Typical/Early) models. The results of these evaluations are documented in Tab. 17, Tab. 18, and Tab. 19.

Table 10. Cross-dataset generalization results of ResNet50 detector trained on different datasets.

Training Dataset	Testing Dataset					Avg
	DiffusionForensics	GenImage	DiffusionDB	ArtiFact	WildFake	
GenImage	84.2/95.6/77.9	99.7/99.9/99.9	93.0/96.3/94.3	61.3/66.1/52.8	71.6/92.1/79.0	81.9/90.0/80.7
DiffusionDB	84.2/84.1/49.4	50.1/49.3/48.5	99.9/100/100	61.3/61.4/50.0	81.1/82.7/72.8	75.3/75.5/64.1
ArtiFact	85.4/94.9/76.7	76.5/84.8/82.9	64.1/69.9/68.1	97.2/99.5/99.3	85.4/94.9/76.7	81.7/88.8/87.4
WildFake	87.2/96.6/83.4	89.0/89.9/89.3	96.3/99.2/99.2	68.0/84.7/75.3	99.6/99.9/99.9	86.4/94.1/89.4

Table 11. Cross-dataset generalization results of ViT detector trained on different datasets.

Training Dataset	Testing Dataset					Avg
	DiffusionForensics	GenImage	DiffusionDB	ArtiFact	WildFake	
GenImage	84.2/97.2/85.3	99.6/99.9/99.9	97.2/99.0/98.6	61.3/61.1/49.8	76.8/93.8/83.3	83.8/90.2/83.4
DiffusionDB	84.2/83.6/47.8	50.0/46.4/42.8	99.9/100/100	61.2/61.5/50.2	80.4/81.9/71.4	75.2/74.6/62.4
ArtiFact	84.2/96.1/82.5	78.5/88.1/85.0	68.4/75.3/73.2	96.8/99.6/99.5	84.2/96.1/82.5	82.4/91.0/84.4
WildFake	95.8/99.1/97.2	88.6/83.6/89.7	99.3/99.8/99.9	62.2/81.9/68.8	99.1/99.9/99.9	89.0/92.8/91.1

Evaluation over Cross-Weight from SD. In open-source communities, users often employ varied training strategies to customize their models. These strategies may include finetuning parts of the base model’s parameters, using the DreamBooth training strategy for optimizing the parameters of UNET or the text-encoder, or creating different adaptors like LORA, ControlNet, and LyCORIS to combine with the base model for controlled generation. To assess how well detectors generalize across different weights within the same SD architecture, we have conducted a cross-weight evaluation. As indicated in Tab. 16, the results show that the ability of detectors to generalize across different weights is on par with their performance in in-weight evaluations.

Evaluation over Cross-version and Cross-Time. Due to the rapid development of DMs, open-source frameworks like SD and commercial entities like Midjourney are updated frequently. To assess the generalization capabilities between typical and advanced generators, we conducted a comprehensive cross-version evaluation. The results for SD are detailed in Tab. 17, and those for Midjourney are in Tab. 18. These cross-version findings suggest that advancements in the quality of fake images have a minimal impact on generalization ability. This phenomenon can be attributed to the fact that the core architecture of these updated generators remains grounded in DMs, and their core modules exhibit stability, leading to relatively consistent characteristics in the generated fake images. Furthermore, we have also compiled cross-time evaluation results for GANs in Tab. 19. These results reveal that detectors trained on the latest GANs display superior generalization capabilities compared to those trained on earlier versions of GANs.

E. Robustness to Degraded Images

Images commonly encounter degradation issues during propagation, such as low resolution, noise interference, and watermarks [64]. It is essential for detectors to exhibit robustness against these challenges. To evaluate the resilience of detectors trained on the WildFake dataset against degraded images, we apply a series of degradation techniques to the images in the testing set:

- DownSample: Reducing the resolution of high-resolution images to either 128 or 64 pixels.
- Compression: Introducing compression artifacts by applying JPEG compression with varying quality ratios to the original test images.
- Geometric Transformation: Randomly flipping or cropping images in the testing set.
- Watermark: Randomly adding textual or visual watermarks to images at various positions in the testing set.
- Color Transformation: Randomly altering the brightness, contrast, saturation, and hue of images from the testing set.

The results of baseline methods evaluated under these degradation conditions on the WildFake dataset are documented in Tab. 20.

Upon analyzing the results, it becomes evident that the ViT-based detector outperforms the ResNet-50-based detector in handling these degraded images. The ResNet-50-based detector is particularly more sensitive to geometric and color transformations, showcasing a higher degree of vulnerability to these specific types of degradation. In contrast, the ViT-based detector exhibits enhanced robustness in the face of such challenges. However, it is noteworthy that both detectors exhibit a reduction in performance when processing images with either image-based or text-based watermarks. Additionally, the experiments reveal that lower

Table 12. Cross-dataset generalization comparison of different detectors trained on GenImage dataset.

Detectors	Testing Dataset					Avg
	DiffusionForensics	GenImage	DiffusionDB	ArtiFact	WildFake	
DIRE	82.9/93.9/76.7	99.5/99.9/99.9	91.3/94.5/92.5	59.1/61.8/52.7	72.1/92.3/80.4	80.9/88.4/80.4
IFDL	86.4/95.9/81.4	99.6/99.9/99.9	93.7/96.8/95.0	61.4/67.4/55.1	74.2/93.7/83.9	83.0/90.7/83.0
Multi-LID	58.8/59.9/51.5	75.8/73.9/74.9	59.1/60.4/52.0	49.9/45.3/42.9	50.5/61.5/54.3	58.8/60.2/55.1
LASTED	87.6/96.2/83.7	99.8/99.9/99.9	94.3/97.9/95.7	63.4/66.7/57.0	78.8/94.3/86.9	84.7/91.0/84.6
ResNet50	84.2/95.6/77.9	99.7/99.9/99.9	93.0/96.3/94.3	61.3/66.1/52.8	71.6/92.1/79.0	81.9/90.0/87.0
ViT	84.2/97.2/85.3	99.6/99.9/99.9	97.2/99.0/98.6	61.3/61.1/49.8	76.8/93.8/83.3	83.8/92.0/83.4

Table 13. Cross-dataset generalization comparison of different detectors trained on DiffusionDB dataset.

Detectors	Testing Dataset					Avg
	DiffusionForensics	GenImage	DiffusionDB	ArtiFact	WildFake	
DIRE	82.7/82.7/53.4	50.0/49.3/47.1	99.9/99.9/99.9	60.3/60.3/50.1	79.1/81.0/72.0	74.4/74.6/64.5
IFDL	88.3/88.1/53.9	52.9/51.8/51.0	99.9/100/100	63.4/62.4/53.5	85.5/85.9/76.5	78.0/77.6/66.9
Multi-LID	50.0/50.8/45.6	47.0/46.5/44.9	77.2/72.4/73.4	49.9/51.9/49.0	51.0/49.4/48.9	55.0/54.2/52.3
LASTED	90.7/90.5/58.4	53.1/53.2/52.3	99.9/100/100	65.4/66.5/55.9	88.2/90.0/79.1	79.4/80.0/69.1
ResNet50	84.2/84.1/49.4	51.0/49.3/48.5	99.9/100/100	61.3/61.4/50.0	81.1/82.7/72.8	75.3/75.5/64.1
ViT	84.2/83.6/47.8	50.0/46.4/42.8	99.9/100/100	61.2/61.5/52.0	84.0/81.9/71.4	75.2/74.6/62.4

resolutions and lower qualities have a significant impact on the accuracy of both types of detectors. This observation underscores the importance of resolution and image quality in the effective functioning of synthetic image detection models.

References

- [1] Agil Aghasanli, Dmitry Kangin, and Plamen Angelov. Interpretable-through-prototypes deepfake detection for diffusion models. In *Proceedings of the IEEE/CVF International Conference on Computer Vision*, pages 467–474, 2023. **1**
- [2] LAION AI. Laion aesthetics v1. technical report version 1.0, 2022. **3**
- [3] Aibek Alanov, Vadim Titov, Maksim Nakhodnov, and Dmitry Vetrov. Styledomain: Efficient and lightweight parameterizations of stylegan for one-shot and few-shot domain adaptation. In *Proceedings of the IEEE/CVF International Conference on Computer Vision*, pages 2184–2194, 2023. **1, 2**
- [4] Antreas Antoniou, Amos Storkey, and Harrison Edwards. Data augmentation generative adversarial networks. *arXiv preprint arXiv:1711.04340*, 2017. **2**
- [5] Martin Arjovsky, Soumith Chintala, and Léon Bottou. Wasserstein generative adversarial networks. In *ICML*, 2017. **2**
- [6] Jianmin Bao, Dong Chen, Fang Wen, Houqiang Li, and Gang Hua. CVAE-GAN: fine-grained image generation through asymmetric training. In *ICCV*, 2017. **3**
- [7] Jordan J Bird and Ahmad Lotfi. Cifake: Image classification and explainable identification of ai-generated synthetic images. *arXiv preprint arXiv:2303.14126*, 2023. **1, 2, 4**
- [8] Andrew Brock, Jeff Donahue, and Karen Simonyan. Large scale gan training for high fidelity natural image synthesis. In *International Conference on Learning Representations*, 2018. **1, 2, 6**
- [9] Huiwen Chang, Han Zhang, Lu Jiang, Ce Liu, and William T Freeman. Maskgit: Masked generative image transformer. In *Proceedings of the IEEE/CVF Conference on Computer Vision and Pattern Recognition*, pages 11315–11325, 2022. **2, 3, 6**
- [10] Huiwen Chang, Han Zhang, Jarred Barber, AJ Maschinot, Jose Lezama, Lu Jiang, Ming-Hsuan Yang, Kevin Murphy, William T Freeman, Michael Rubinstein, et al. Muse: Text-to-image generation via masked generative transformers. *arXiv preprint arXiv:2301.00704*, 2023. **2, 3, 6**
- [11] Yunjey Choi, Minje Choi, Munyoung Kim, Jung-Woo Ha, Sunghun Kim, and Jaegul Choo. Stargan: Unified generative adversarial networks for multi-domain image-to-image translation. In *Proceedings of the IEEE conference on computer vision and pattern recognition*, pages 8789–8797, 2018. **2, 6**
- [12] Yunjey Choi, Youngjung Uh, Jaejun Yoo, and Jung-Woo Ha. Stargan v2: Diverse image synthesis for multiple domains. In *Proceedings of the IEEE/CVF conference on computer vision and pattern recognition*, pages 8188–8197, 2020. **1, 2, 6**
- [13] Riccardo Corvi, Davide Cozzolino, Giada Zingarini, Giovanni Poggi, Koki Nagano, and Luisa Verdoliva. On the detection of synthetic images generated by diffusion models. In *ICASSP 2023-2023 IEEE International Conference on Acoustics, Speech and Signal Processing (ICASSP)*, pages 1–5. IEEE, 2023. **1**
- [14] Jia Deng, Wei Dong, Richard Socher, Li-Jia Li, Kai Li, and Li Fei-Fei. Imagenet: A large-scale hierarchical image

Table 14. Cross-dataset generalization comparison of different detectors trained on ArtiFact dataset.

Detectors	Testing Dataset					Avg
	DiffusionForensics	GenImage	DiffusionDB	ArtiFact	WildFake	
DIRE	79.5/88.3/74.6	75.4/82.0/82.3	59.9/64.8/62.5	92.4/92.6/92.4	69.8/83.4/70.2	75.4/82.2/76.4
IFDL	87.9/95.8/80.0	78.3/87.1/84.9	66.2/72.1/69.1	97.6/99.6/99.6	71.9/90.0/75.5	80.3/88.9/81.8
Multi-LID	55.7/61.4/54.7	53.6/59.6/58.4	49.9/50.9/49.7	71.0/72.7/73.5	50.8/59.7/51.9	56.2/60.9/57.4
LASTED	91.3/98.6/84.1	80.2/89.1/89.2	69.5/75.7/72.6	98.2/99.7/99.6	73.0/92.0/77.8	82.4/91.1/84.7
ResNet50	85.4/94.9/76.7	76.5/84.8/82.9	64.1/69.9/68.1	97.2/99.5/99.3	85.4/94.9/76.7	81.7/88.8/87.4
ViT	84.2/96.1/82.5	78.5/88.1/85.0	68.4/75.3/73.2	96.8/99.6/99.5	84.2/96.1/82.5	82.4/91.0/84.4

Table 15. Cross-dataset generalization comparison of different detectors trained on the proposed WildFake dataset.

Detectors	Testing Dataset					Avg
	DiffusionForensics	GenImage	DiffusionDB	ArtiFact	WildFake	
DIRE	85.5/97.5/84.9	77.3/85.1/84.5	97.2/99.3/99.3	67.6/84.0/74.8	89.3/89.6/89.7	83.4/91.1/86.6
IFDL	88.6/97.9/92.8	85.1/95.0/89.9	97.7/99.5/99.7	67.7/82.1/72.4	99.3/99.9/99.9	87.6/93.9/99.0
Multi-LID	56.7/58.8/54.4	52.1/58.2/58.1	62.1/64.5/64.6	51.2/55.1/56.0	74.3/75.9/75.9	59.2/62.5/61.8
LASTED	94.9/98.1/96.2	87.0/91.4/93.8	98.9/99.7/99.8	71.4/89.0/79.1	99.7/99.9/99.9	93.0/95.6/93.7
ResNet50	87.2/96.6/83.4	89.0/89.9/89.3	96.3/99.2/99.2	68.0/84.7/75.3	99.6/99.9/99.9	86.4/94.1/89.4
ViT	95.8/99.1/97.2	88.6/83.6/89.7	99.3/99.8/99.9	62.2/81.9/68.8	99.1/99.9/99.9	89.0/92.8/91.1

Table 16. Results of cross-weight from SD evaluation on different training and testing subsets using ViT.

Training Subset	Testing Subset		
	Original SD	Personalized SD	SD with Adaptor
Original SD	99.9/100/99.9	99.8/99.9/99.9	99.8/99.9/99.9
Personalized SD	99.7/99.9/99.8	99.9/99.9/99.9	99.8/99.9/99.9
SD with Adaptor	99.9/99.9/99.9	99.9/99.9/99.9	99.9/99.9/99.9

Table 17. Results of cross-version evaluation over SD from DMs generators using ViT.

Training Subset	Testing Subset	
	Advanced	Typical
Advanced	100/100/99.9	99.5/99.9/99.9
Typical	99.9/99.9/99.9	99.9/99.9/99.9

Table 18. Results of cross-version evaluation over Midjourney from DMs generators using ViT.

Training Subset	Testing Subset	
	Advanced	Typical
Advanced	99.5/99.9/99.9	99.5/99.9/99.9
Typical	99.9/99.9/99.9	99.9/99.9/100

database. In *2009 IEEE conference on computer vision and pattern recognition*, pages 248–255. IEEE, 2009. 6

- [15] Prafulla Dhariwal and Alexander Nichol. Diffusion models beat gans on image synthesis. *Advances in neural information processing systems*, 34:8780–8794, 2021. 3, 6, 9

Table 19. Results of cross-time evaluation over GANs generators using ViT.

Training Subset	Testing Subset	
	Latest	Early
Latest	99.9/100/100	81.1/39.4/64.3
Early	66.6/67.8/51.1	97.5/96.6/99.2

- [16] Laurent Dinh, Jascha Sohl-Dickstein, and Samy Bengio. Density estimation using real nvp. *arXiv preprint arXiv:1605.08803*, 2016. 3
- [17] Carl Doersch. Tutorial on variational autoencoders. *arXiv preprint arXiv:1606.05908*, 2016. 3
- [18] Alexey Dosovitskiy, Lucas Beyer, Alexander Kolesnikov, Dirk Weissenborn, Xiaohua Zhai, Thomas Unterthiner, Mostafa Dehghani, Matthias Minderer, Georg Heigold, Sylvain Gelly, et al. An image is worth 16x16 words: Transformers for image recognition at scale. In *International Conference on Learning Representations*, 2020. 7, 9, 10, 11
- [19] Patrick Esser, Robin Rombach, and Bjorn Ommer. Taming transformers for high-resolution image synthesis. In *Proceedings of the IEEE/CVF conference on computer vision and pattern recognition*, pages 12873–12883, 2021. 1, 2, 3, 6
- [20] Joel Frank, Thorsten Eisenhofer, Lea Schönherr, Asja Fischer, Dorothea Kolossa, and Thorsten Holz. Leveraging frequency analysis for deep fake image recognition. In *International conference on machine learning*, pages 3247–3258. PMLR, 2020. 1
- [21] Rinon Gal, Yuval Alaluf, Yuval Atzmon, Or Patashnik, Amit Haim Bermano, Gal Chechik, and Daniel Cohen-or. An

Table 20. Robustness evaluation of different detectors trained on the proposed WildFake dataset. “Trans” denotes Transformation.

Method	DownSample		Compression		Geometric Transformation		Watermarks		Color Trans
	128	64	q=70	q=35	Flip	Crop	Text	Image	
DIRE	85.8/88.9/87.6	61.6/56.3/33.9	75.6/82.7/81.0	65.4/75.5/71.2	85.0/91.8/89.3	86.3/92.5/91.6	87.7/94.2/90.6	86.5/93.8/89.4	81.3/89.1/86.8
IFDL	91.3/95.2/93.4	73.1/69.6/49.4	87.4/97.8/95.1	82.9/94.1/89.3	94.1/99.4/98.2	94.9/99.6/99.1	93.8/99.3/96.9	91.3/99.1/94.9	96.0/98.2/97.1
Multi-LID	59.3/62.4/61.5	51.3/50.2/35.8	55.7/58.6/57.5	53.3/56.8/54.6	58.9/64.1/61.6	59.5/64.4/63.3	60.0/61.2/59.1	58.0/62.2/59.0	58.3/59.4/61.6
LASTED	92.5/96.5/93.2	75.8/71.3/51.8	89.6/97.7/95.0	88.5/95.7/91.5	96.1/99.3/99.0	98.0/99.6/99.6	95.4/99.4/97.6	94.7/99.5/97.4	92.3/99.8/99.6
ResNet50	91.1/95.5/93.1	71.3/65.0/39.8	84.6/95.9/92.5	85.0/93.1/87.7	95.1/98.4/96.4	91.3/98.7/96.9	91.0/98.8/94.1	90.8/98.8/93.9	87.9/97.3/94.8
ViT	91.8/94.6/92.4	79.3/78.2/66.2	92.4/98.1/96.0	86.6/95.1/95.0	97.1/99.8/99.4	98.9/99.9/99.1	93.6/99.3/96.6	92.9/99.3/96.5	98.5/99.9/99.8

image is worth one word: Personalizing text-to-image generation using textual inversion. In *The Eleventh International Conference on Learning Representations*, 2022. 6

- [22] Ian Goodfellow, Jean Pouget-Abadie, Mehdi Mirza, Bing Xu, David Warde-Farley, Sherjil Ozair, Aaron Courville, and Yoshua Bengio. Generative adversarial nets. In *NeurIPS*, 2014. 2
- [23] Jiayi Gu, Xiaojun Meng, Guansong Lu, Lu Hou, Niu Minzhe, Xiaodan Liang, Lewei Yao, Runhui Huang, Wei Zhang, Xin Jiang, et al. Wukong: A 100 million large-scale chinese cross-modal pre-training benchmark. *Advances in Neural Information Processing Systems*, 35:26418–26431, 2022. 6
- [24] Shuyang Gu, Dong Chen, Jianmin Bao, Fang Wen, Bo Zhang, Dongdong Chen, Lu Yuan, and Baining Guo. Vector quantized diffusion model for text-to-image synthesis. In *Proceedings of the IEEE/CVF Conference on Computer Vision and Pattern Recognition*, pages 10696–10706, 2022. 2, 3, 6
- [25] Xiao Guo, Xiaohong Liu, Zhiyuan Ren, Steven Grosz, Iacopo Masi, and Xiaoming Liu. Hierarchical fine-grained image forgery detection and localization. In *Proceedings of the IEEE/CVF Conference on Computer Vision and Pattern Recognition*, pages 3155–3165, 2023. 5, 7, 9, 10, 11
- [26] Kaiming He, Xiangyu Zhang, Shaoqing Ren, and Jian Sun. Deep residual learning for image recognition. In *Proceedings of the IEEE conference on computer vision and pattern recognition*, pages 770–778, 2016. 4, 7, 9, 10, 11
- [27] Kaiming He, Xinlei Chen, Saining Xie, Yanghao Li, Piotr Dollár, and Ross Girshick. Masked autoencoders are scalable vision learners. In *Proceedings of the IEEE/CVF conference on computer vision and pattern recognition*, pages 16000–16009, 2022. 3
- [28] hello@civitai.com. civitai, 2022. 6
- [29] Irina Higgins, Loic Matthey, Arka Pal, Christopher Burgess, Xavier Glorot, Matthew Botvinick, Shakir Mohamed, and Alexander Lerchner. beta-vae: Learning basic visual concepts with a constrained variational framework. In *International conference on learning representations*, 2016. 3
- [30] Jonathan Ho, Ajay Jain, and Pieter Abbeel. Denoising diffusion probabilistic models. *Advances in neural information processing systems*, 33:6840–6851, 2020. 2, 3, 6
- [31] Oleksii Holub. Discordchatexporter, 2017. 4, 10
- [32] Oleksii Holub. Midjourney, 2022. 2, 3, 6
- [33] Edward J Hu, Yelong Shen, Phillip Wallis, Zeyuan Allen-Zhu, Yuanzhi Li, Shean Wang, Lu Wang, and Weizhu Chen. Lora: Low-rank adaptation of large language models. *arXiv preprint arXiv:2106.09685*, 2021. 6
- [34] Mengqi Huang, Zhendong Mao, Zhuowei Chen, and Yongdong Zhang. Towards accurate image coding: Improved autoregressive image generation with dynamic vector quantization. In *Proceedings of the IEEE/CVF Conference on Computer Vision and Pattern Recognition*, pages 22596–22605, 2023. 2
- [35] Mengqi Huang, Zhendong Mao, Quan Wang, and Yongdong Zhang. Not all image regions matter: Masked vector quantization for autoregressive image generation. In *Proceedings of the IEEE/CVF Conference on Computer Vision and Pattern Recognition*, pages 2002–2011, 2023. 2
- [36] Minguk Kang, Jun-Yan Zhu, Richard Zhang, Jaesik Park, Eli Shechtman, Sylvain Paris, and Taesung Park. Scaling up gans for text-to-image synthesis. In *Proceedings of the IEEE/CVF Conference on Computer Vision and Pattern Recognition*, pages 10124–10134, 2023. 1, 2, 6
- [37] Tero Karras, Timo Aila, Samuli Laine, and Jaakko Lehtinen. Progressive growing of gans for improved quality, stability, and variation. *arXiv preprint arXiv:1710.10196*, 2017. 4, 6, 10
- [38] Tero Karras, Samuli Laine, and Timo Aila. A style-based generator architecture for generative adversarial networks. In *Proceedings of the IEEE/CVF conference on computer vision and pattern recognition*, pages 4401–4410, 2019. 1, 2, 6
- [39] Tero Karras, Samuli Laine, Miika Aittala, Janne Hellsten, Jaakko Lehtinen, and Timo Aila. Analyzing and improving the image quality of stylegan. In *Proceedings of the IEEE/CVF conference on computer vision and pattern recognition*, pages 8110–8119, 2020.
- [40] Tero Karras, Miika Aittala, Samuli Laine, Erik Härkönen, Janne Hellsten, Jaakko Lehtinen, and Timo Aila. Alias-free generative adversarial networks. *Advances in Neural Information Processing Systems*, 34:852–863, 2021. 2, 6
- [41] Diederik P Kingma and Jimmy Ba. Adam: A method for stochastic optimization. *arXiv preprint arXiv:1412.6980*, 2014. 9
- [42] Durk P Kingma and Prafulla Dhariwal. Glow: Generative flow with invertible 1x1 convolutions. *Advances in neural information processing systems*, 31, 2018. 3
- [43] Diederik P Kingma and Max Welling. Auto-encoding variational bayes. *arXiv preprint arXiv:1312.6114*, 2013. 3
- [44] Alex Krizhevsky, Geoffrey Hinton, et al. Learning multiple layers of features from tiny images. 2009. 4

- [45] Tianhong Li, Huiwen Chang, Shlok Mishra, Han Zhang, Dina Katabi, and Dilip Krishnan. Mage: Masked generative encoder to unify representation learning and image synthesis. In *Proceedings of the IEEE/CVF Conference on Computer Vision and Pattern Recognition*, pages 2142–2152, 2023. [2](#), [3](#)
- [46] Tsung-Yi Lin, Michael Maire, Serge Belongie, James Hays, Pietro Perona, Deva Ramanan, Piotr Dollár, and C Lawrence Zitnick. Microsoft coco: Common objects in context. In *Computer Vision–ECCV 2014: 13th European Conference, Zurich, Switzerland, September 6–12, 2014, Proceedings, Part V 13*, pages 740–755. Springer, 2014. [4](#), [6](#)
- [47] Peter Lorenz, Ricard L Durall, and Janis Keuper. Detecting images generated by deep diffusion models using their local intrinsic dimensionality. In *Proceedings of the IEEE/CVF International Conference on Computer Vision*, pages 448–459, 2023. [1](#), [5](#), [7](#), [9](#), [10](#), [11](#)
- [48] Francesco Marra, Diego Gragnaniello, Davide Cozzolino, and Luisa Verdoliva. Detection of gan-generated fake images over social networks. In *2018 IEEE conference on multimedia information processing and retrieval (MIPR)*, pages 384–389. IEEE, 2018. [1](#)
- [49] Francesco Marra, Diego Gragnaniello, Luisa Verdoliva, and Giovanni Poggi. Do gans leave artificial fingerprints? In *2019 IEEE conference on multimedia information processing and retrieval (MIPR)*, pages 506–511. IEEE, 2019. [1](#)
- [50] Alexander Quinn Nichol, Prafulla Dhariwal, Aditya Ramesh, Pranav Shyam, Pamela Mishkin, Bob McGrew, Ilya Sutskever, and Mark Chen. Glide: Towards photorealistic image generation and editing with text-guided diffusion models. In *International Conference on Machine Learning*, pages 16784–16804. PMLR, 2022. [2](#)
- [51] OpenAI. Dall-e 3 system card, 2023. [2](#), [3](#)
- [52] Niki Parmar, Ashish Vaswani, Jakob Uszkoreit, Lukasz Kaiser, Noam Shazeer, Alexander Ku, and Dustin Tran. Image transformer. In *ICML*, 2018. [4](#)
- [53] Hamza Pehlivan, Yusuf Dalva, and Aysegul Dunder. Styleres: Transforming the residuals for real image editing with stylegan. In *Proceedings of the IEEE/CVF Conference on Computer Vision and Pattern Recognition*, pages 1828–1837, 2023. [1](#), [2](#)
- [54] Alec Radford, Jong Wook Kim, Chris Hallacy, Aditya Ramesh, Gabriel Goh, Sandhini Agarwal, Girish Sastry, Amanda Askell, Pamela Mishkin, Jack Clark, et al. Learning transferable visual models from natural language supervision. In *International conference on machine learning*, pages 8748–8763. PMLR, 2021. [7](#)
- [55] Md Awsafur Rahman, Bishmoy Paul, Najibul Haque Sarker, Zaber Ibn Abdul Hakim, and Shaikh Anowarul Fattah. Artifact: A large-scale dataset with artificial and factual images for generalizable and robust synthetic image detection. *arXiv preprint arXiv:2302.11970*, 2023. [1](#), [2](#), [4](#), [6](#), [7](#), [10](#), [11](#)
- [56] Aditya Ramesh, Prafulla Dhariwal, Alex Nichol, Casey Chu, and Mark Chen. Hierarchical text-conditional image generation with clip latents. [2](#), [3](#), [6](#)
- [57] Ali Razavi, Aaron Van den Oord, and Oriol Vinyals. Generating diverse high-fidelity images with vq-vae-2. *Advances in neural information processing systems*, 32, 2019. [2](#)
- [58] Danilo Rezende and Shakir Mohamed. Variational inference with normalizing flows. In *International conference on machine learning*, pages 1530–1538. PMLR, 2015. [3](#)
- [59] Robin Rombach, Andreas Blattmann, Dominik Lorenz, Patrick Esser, and Björn Ommer. High-resolution image synthesis with latent diffusion models. In *Proceedings of the IEEE/CVF conference on computer vision and pattern recognition*, pages 10684–10695, 2022. [1](#), [2](#), [3](#), [4](#), [6](#)
- [60] Nataniel Ruiz, Yuanzhen Li, Varun Jampani, Yael Pritch, Michael Rubinstein, and Kfir Aberman. Dreambooth: Fine tuning text-to-image diffusion models for subject-driven generation. In *Proceedings of the IEEE/CVF Conference on Computer Vision and Pattern Recognition*, pages 22500–22510, 2023. [6](#)
- [61] Olga Russakovsky, Jia Deng, Hao Su, Jonathan Krause, Sanjeev Satheesh, Sean Ma, Zhiheng Huang, Andrej Karpathy, Aditya Khosla, Michael Bernstein, et al. Imagenet: large scale visual recognition challenge. *IJCV*, 115(3):211–252, 2015. [4](#), [10](#)
- [62] Chitwan Saharia, William Chan, Saurabh Saxena, Lala Li, Jay Whang, Emily L Denton, Kamyar Ghasemipour, Raphael Gontijo Lopes, Burcu Karagol Ayan, Tim Salimans, et al. Photorealistic text-to-image diffusion models with deep language understanding. *Advances in Neural Information Processing Systems*, 35:36479–36494, 2022. [1](#), [2](#), [3](#), [6](#)
- [63] Axel Sauer, Katja Schwarz, and Andreas Geiger. Stylegan-xl: Scaling stylegan to large diverse datasets. In *ACM SIGGRAPH 2022 conference proceedings*, pages 1–10, 2022. [1](#), [2](#)
- [64] Raimondo Schettini and Silvia Corchs. Underwater image processing: state of the art of restoration and image enhancement methods. *EURASIP journal on advances in signal processing*, 2010:1–14, 2010. [8](#), [12](#)
- [65] Christoph Schuhmann, Romain Beaumont, Richard Vencu, Cade Gordon, Ross Wightman, Mehdi Cherti, Theo Coombes, Aarush Katta, Clayton Mullis, Mitchell Wortsman, et al. Laion-5b: An open large-scale dataset for training next generation image-text models. *Advances in Neural Information Processing Systems*, 35:25278–25294, 2022. [6](#)
- [66] Zeyang Sha, Zheng Li, Ning Yu, and Yang Zhang. De-fake: Detection and attribution of fake images generated by text-to-image diffusion models. *arXiv preprint arXiv:2210.06998*, 2022. [1](#), [2](#), [4](#)
- [67] Jiaming Song, Chenlin Meng, and Stefano Ermon. Denoising diffusion implicit models. In *International Conference on Learning Representations*, 2020. [2](#), [3](#), [6](#), [9](#)
- [68] Ming Tao, Hao Tang, Fei Wu, Xiao-Yuan Jing, Bing-Kun Bao, and Changsheng Xu. Df-gan: A simple and effective baseline for text-to-image synthesis. In *Proceedings of the IEEE/CVF Conference on Computer Vision and Pattern Recognition*, pages 16515–16525, 2022. [1](#), [2](#), [6](#)
- [69] Ming Tao, Bing-Kun Bao, Hao Tang, and Changsheng Xu. Galip: Generative adversarial clips for text-to-image synthesis. In *Proceedings of the IEEE/CVF Conference on Computer Vision and Pattern Recognition*, pages 14214–14223, 2023. [1](#), [2](#), [6](#)
- [70] Aaron Van Den Oord, Oriol Vinyals, et al. Neural discrete

- representation learning. *Advances in neural information processing systems*, 30, 2017. 2, 3, 6
- [71] Luisa Verdoliva, Davide Cozzolino, and Koki Nagano. 2022 ieeecup image and video processing cup synthetic image detection. 1, 2, 4
- [72] Andrey Voynov, Qinghao Chu, Daniel Cohen-Or, and Kfir Aberman. $p+$: Extended textual conditioning in text-to-image generation. *arXiv preprint arXiv:2303.09522*, 2023. 6
- [73] Sheng-Yu Wang, Oliver Wang, Andrew Owens, Richard Zhang, and Alexei A Efros. Detecting photoshopped faces by scripting photoshop. In *Proceedings of the IEEE/CVF International Conference on Computer Vision*, pages 10072–10081, 2019. 7
- [74] Sheng-Yu Wang, Oliver Wang, Richard Zhang, Andrew Owens, and Alexei A Efros. Cnn-generated images are surprisingly easy to spot... for now. In *Proceedings of the IEEE/CVF conference on computer vision and pattern recognition*, pages 8695–8704, 2020. 1, 2, 4, 7
- [75] Zhendong Wang, Jianmin Bao, Wengang Zhou, Weilun Wang, Hezhen Hu, Hong Chen, and Houqiang Li. Dire for diffusion-generated image detection. *arXiv preprint arXiv:2303.09295*, 2023. 1, 2, 4, 6, 7, 9, 10, 11
- [76] Zijie J Wang, Evan Montoya, David Munechika, Haoyang Yang, Benjamin Hoover, and Duen Horng Chau. Diffusiondb: A large-scale prompt gallery dataset for text-to-image generative models. *arXiv preprint arXiv:2210.14896*, 2022. 1, 2, 4, 6, 9, 10, 11
- [77] Haiwei Wu, Jiantao Zhou, and Shile Zhang. Generalizable synthetic image detection via language-guided contrastive learning. *arXiv preprint arXiv:2305.13800*, 2023. 1, 5, 7, 9, 10, 11
- [78] Shin-Ying Yeh, Yu-Guan Hsieh, Zhidong Gao, Bernard BW Yang, Giyeong Oh, and Yanmin Gong. Navigating text-to-image customization: From lycoris fine-tuning to model evaluation. *arXiv preprint arXiv:2309.14859*, 2023. 6
- [79] Peter Young, Alice Lai, Micah Hodosh, and Julia Hockenmaier. From image descriptions to visual denotations: New similarity metrics for semantic inference over event descriptions. *Transactions of the Association for Computational Linguistics*, 2:67–78, 2014. 4
- [80] Fisher Yu, Ari Seff, Yinda Zhang, Shuran Song, Thomas Funkhouser, and Jianxiong Xiao. Lsun: Construction of a large-scale image dataset using deep learning with humans in the loop. *arXiv preprint arXiv:1506.03365*, 2015. 4, 6, 9, 10
- [81] Jianfu Zhang, Yuanyuan Huang, Yaoyi Li, Weijie Zhao, and Liqing Zhang. Multi-attribute transfer via disentangled representation. In *AAAI*, 2019. 2
- [82] Lvmin Zhang, Anyi Rao, and Maneesh Agrawala. Adding conditional control to text-to-image diffusion models. In *Proceedings of the IEEE/CVF International Conference on Computer Vision*, pages 3836–3847, 2023. 6
- [83] Jun-Yan Zhu, Taesung Park, Phillip Isola, and Alexei A Efros. Unpaired image-to-image translation using cycle-consistent adversarial networks. In *Proceedings of the IEEE international conference on computer vision*, pages 2223–2232, 2017. 2
- [84] Mingjian Zhu, Hanting Chen, Qiangyu Yan, Xudong Huang, Guanyu Lin, Wei Li, Zhijun Tu, Hailin Hu, Jie Hu, and Yunhe Wang. Genimage: A million-scale benchmark for detecting ai-generated image. *arXiv preprint arXiv:2306.08571*, 2023. 1, 2, 4, 6, 7, 10, 11